



# Investigations of crystallization behaviour of $\text{Co}_{80}\text{Si}_9\text{B}_{11}$ amorphous alloy

S. Lesz<sup>a,\*</sup>, R. Nowosielski<sup>a</sup>, A. Zajdel<sup>a</sup>, B. Kostrubiec<sup>b</sup>, Z. Stokłosa<sup>b</sup>

<sup>a</sup> Division of Nanocrystalline and Functional Materials and Sustainable Pro-ecological Technologies, Institute of Engineering Materials and Biomaterials, Silesian University of Technology, ul. Konarskiego 18a, 44-100 Gliwice, Poland

<sup>b</sup> Institute of Materials Science, Silesian University, ul. Bankowa 12, 40-007 Katowice, Poland

\* Corresponding author: E-mail address: sabina.lesz@polsl.pl

Received 31.03.2006; accepted in revised form 25.01.2007

## ABSTRACT

**Purpose:** This paper describes crystallization kinetics and changes of magnetic properties involved by process of crystallization of the amorphous  $\text{Co}_{80}\text{Si}_9\text{B}_{11}$  alloy.

**Design/methodology/approach:** The following experimental techniques were used: X-ray diffraction (XRD), electrical resistivity in situ measurements (four-point probe), static and dynamic measurements of magnetic properties (magnetic balance, fluxmeter, Maxwell-Wien bridge).

**Findings:** In this work has been performed influence of thermal annealing on crystallization kinetics and magnetic properties amorphous  $\text{Co}_{80}\text{Si}_9\text{B}_{11}$  alloy.

**Practical implications:** The attractive properties of Co-Si-B alloy are of special interest for basic research on the materials as well as for their potential applications, like magnetic sensors. The Co soft magnetic material is used in noise filters, saturable reactors, miniature inductance elements for abating spike noise, mains transformers, choke coils, zero-phase current transformers, and magnetic heads etc., i.e., devices which are expected to exhibit high levels of permeability at high frequencies.

**Originality/value:** It has been shown that thermal annealing at temperature close to the crystallization temperature leads to a significant increase of the initial magnetic permeability. The maximum permeability for examined alloy in as quenched state is about 11300.

**Keywords:** Materials; Amorphous Materials; Nanomaterials; Heat treatment; Crystallization behavior; Magnetic properties

## PROPERTIES

### 1. Introduction

Amorphous alloys can be prepared by various techniques, including melt spinning [1-4], mechanical alloying [5-8] vapor deposition, chemical alloying [9], etc.

The melt spinning technique allows the rapid solidification of metallic alloys to produce amorphous or nanocrystalline material [3,4].

Alloys of the binary Co-B system can easily be amorphized by melt spinning. More complex alloys with specific properties can be obtained by adding other elements to this system and various chemical compounds can be crystallized from the amorphous phase at specific temperatures [10].

Both Fe-based as well as Co-based amorphous materials have good soft magnetic properties, such as high saturation magnetization, high permeability, low coercivity and loss, which find their applications in antitheft security system, power

electronics, telecommunication devices and automotive magnetics [1-3,9,11,12]. Permeability as well as core-losses can be developed by a further heat treatment. In the heat treatment, the material is typically heated to a specific temperature in an inert atmosphere for a certain time [13-15]. The heat treatment can be realized by impulse methods, too [16,17]. The method most often used is isothermal heating in constant time, for instance 0.5, 1.0, 1.5, 4.0, 8.0 hour [4,18÷21].

For this reasons they have been the subject of much scientific research over the past few decades. In addition to the excellent magnetic properties, the magnetic amorphous alloys present a new system through which crystallization process and corresponding changes in magnetic properties can be systematically studied [13-15]. The kinetics of crystallization of metallic glasses is often described by the well-known phenomenological Johnson-Mehl-Avrami equation for isothermal experiments [2,20,21]. The activation energy of the crystallization process can be obtained from the temperature dependence of the reaction-rate constant, which is known as Kissinger's method [14,15,20÷22].

Our recent researches have focused on crystallization behavior of  $\text{Co}_{80}\text{Si}_9\text{B}_{11}$  amorphous alloy induced by thermal treatment. In this paper, the results obtained on amorphous  $\text{Co}_{80}\text{Si}_9\text{B}_{11}$  alloy heat treated at different temperatures are presented and discussed.

## 2. Experiments

Amorphous  $\text{Co}_{80}\text{Si}_9\text{B}_{11}$  alloy investigated in the present paper was obtained by melt spinning technique as the form of strip 7 mm wide and 14  $\mu\text{m}$  thickness. In order to verify the chemical composition the X-ray fluorescence (XRF) method was used (SPEUPERPROBE 733 JEOL). The samples in the as quenched state were preliminary annealed by 1h and 0,5 h in the temperature range 373-873 K with step of 50 K. Structural investigations were carried out by applying the X-ray diffraction (XRD) method (XRD7, SEIFERTFPM with filtered  $\text{Co-K}\alpha$  radiation) for samples in the as quenched state and after annealing. The parameters of diffractometer are listed in Table 1.

For samples in the as quenched state, the relative magnetic permeability (Maxwell-Wien bridge, frequency 1 kHz, magnetic field 0.5 A/m), saturation magnetization and maximum of the permeability (fluxmeter) at room temperature were obtained. Relative magnetic permeability in weak magnetic field was also determined at room temperature for samples after annealing at  $T_a$  temperatures.

Kinetics of the crystallization process was examined by applying electrical resistivity  $\rho(T)$  (four point probe) and saturation magnetization  $M(T)$  (magnetic balance) measurements in situ with heating rates from 0.5K/min to 10.0 K/min.

The crystallization temperature  $T_{x1}$ , and the activation energy of the crystallization process  $E_c$  from the isochronal resistivity curves were determined. The temperature  $T_{x1}$  can be obtained from the condition  $d\rho/dT=0$ . The effective activation energy  $E_c$  was evaluated by the Kissinger method [20,22], which can be described:

$$\ln \frac{V_l}{T_h^2} + \ln \text{const} = -\frac{E_c}{k_B} \cdot \frac{1}{T_h} \quad (1)$$

where:  $E_c$  is the effective activation energy for the crystallization processes,  $V_l$  - is linear heating rate,  $T_h$  - is the so-called temperature of an homological point determined for the heating rate  $V_l$ , i.e. temperature which the rate of crystallization process is maximum [20,23], and  $k_B$  is the Boltzman constant.

Results obtained from  $M(T)$  measurements were presented as normalized  $M(T)/M(300 \text{ K})$  curves.

Table 1.

The diffractometer's parameters used in XRD method for samples of  $\text{Co}_{80}\text{Si}_9\text{B}_{11}$  alloy

Diffractometer's parameters	Diffractometer XRD 7, SEIFERT - FPM firm	
	a	b
Current intensity of X – ray tube	40 mA	40 mA
Voltage of X – ray tube	35 kV	35 kV
The time of counting in one measurement's point	7s	20s
Step between measurement's points	0.05° $\Theta$	0.01° $\Theta$

## 3. Results and discussion

The examinations of structure performed by X-ray diffraction (XRD) technique show that in as quenched state  $\text{Co}_{80}\text{Si}_9\text{B}_{11}$  alloy has amorphous structure (Fig. 1).

Only a broad diffraction peak at about  $2\Theta \approx 52^\circ$  can be observed from Fig. 1, indicating that obtained ribbon had amorphous structure.

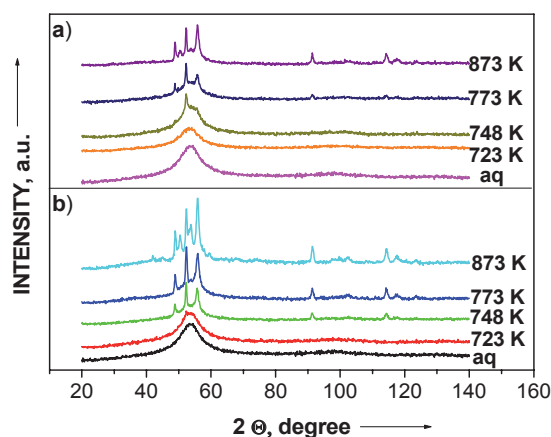


Fig. 1. X-ray diffraction pattern of the  $\text{Co}_{80}\text{Si}_9\text{B}_{11}$  alloy in as quenched state and after annealing in temperature range  $T_a=723\div 873\text{K}$  for 0.5 h (a) and 1.0 h (b). The diffractometer's parameters – see Table 1 (a)

The investigated  $\text{Co}_{80}\text{Si}_9\text{B}_{11}$  alloy in as quenched state has a following properties: high value of resistivity  $\rho$  equal  $1.15 \mu\Omega\text{m}$  (Fig. 2), saturation magnetization  $M=0.9 \text{ T}$  (Fig. 3), initial relative magnetic permeability  $\mu_r=1090$  (Table 2) and  $\mu_{max}=11300$  (Fig. 4).

The obtained physical properties, i.e.  $\rho$ ,  $M$ ,  $\mu_r$  and  $\mu_{max}$  allow to classify the  $\text{Co}_{80}\text{Si}_9\text{B}_{11}$  alloy in as quenched state as a soft magnetic material.

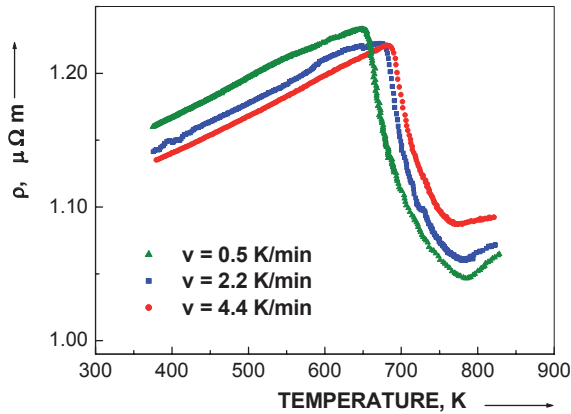


Fig. 2. The in situ isochronal resistivity curves for  $\text{Co}_{80}\text{Si}_9\text{B}_{11}$  alloy obtained with heating rate 0.5, 2.2 and 4.4 K/min

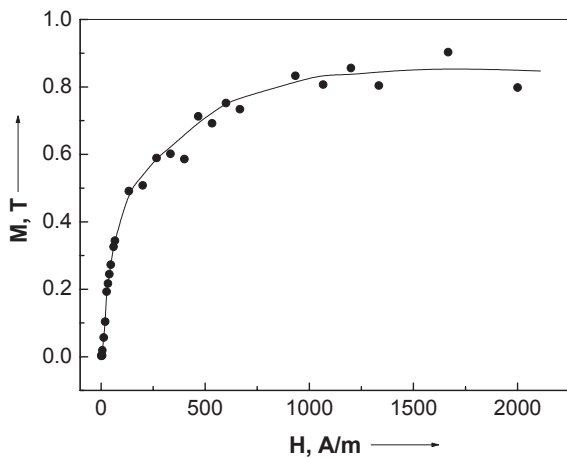


Fig. 3. Magnetization  $M$  versus magnetic field for amorphous  $\text{Co}_{80}\text{Si}_9\text{B}_{11}$  alloy in as quenched state obtained by magnetic balance

There are three types of crystallization transformations for amorphous alloys: primary, polymorphous and eutectic [4].

The different methods (both isothermal and non-isothermal) were used for determining of crystallization temperatures (primary crystallization temperature -  $T_{x1}$  and secondary crystallization temperature -  $T_{x2}$ ) of  $\text{Co}_{80}\text{Si}_9\text{B}_{11}$  alloy.

In order to determine the characteristic temperature of the first ( $T_{x1}$ ) and second ( $T_{x2}$ ) stage of crystallization process electrical

resistivity measurements with continuous heating rate in the range from  $0.5\div 10 \text{ K/min}$  were used.

From Fig. 2 and 5 shows that value of the crystallization temperature  $T_{x1}$  is dependent of the heating rate and is in the range of  $655\div 681 \text{ K}$  for the heating rate  $0.5\div 4.4 \text{ K/min}$ , respectively.

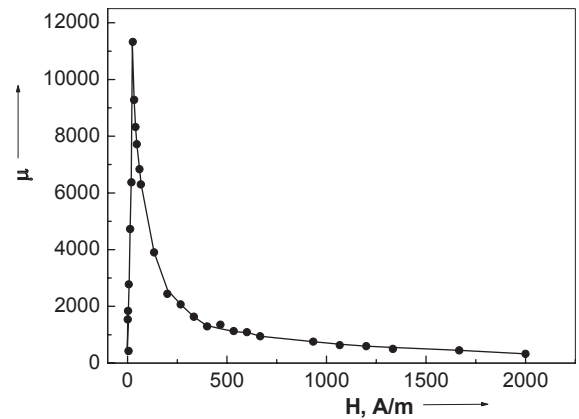


Fig. 4. The maximum permeability  $\mu_{max}$  for amorphous  $\text{Co}_{80}\text{Si}_9\text{B}_{11}$  alloy in as quenched state obtained by magnetic balance

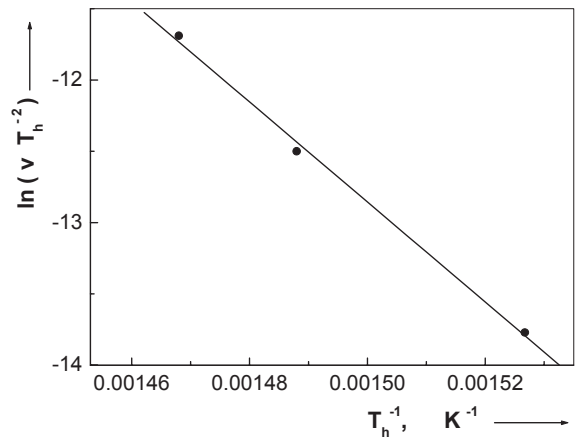


Fig. 5. Plot of  $\ln(v/T_h^2)$  versus  $T_h^{-1}$  for  $\text{Co}_{80}\text{Si}_9\text{B}_{11}$  alloy (see Fig. 2)

Fig 5 shows the plot  $\ln(v/T_h^2)$  versus  $T_h^{-1}$ , which according to Eq. (1) allows determining the activation energy  $E_c$ .

The activation energy  $E_c$  for crystallization of  $\text{Co}_{80}\text{Si}_9\text{B}_{11}$  is calculated to be  $3.0\pm 0.2 \text{ eV}$  [14,24]. As an example in Fig. 6 a and 7 a we present  $\rho(T)$  curves obtained for  $\text{Co}_{80}\text{Si}_9\text{B}_{11}$  alloy with heating rate 5 and 10 K/min, respectively. Fig. 6 b and 7 b represent  $d\rho(T)/dT$  curves from which the temperatures of the first ( $T_{x1}$ ) and second ( $T_{x2}$ ) stage of crystallization process can be determined from the condition  $d\rho(T)/dT=0$ . From Fig. 6 b and 7 b shows that characteristic temperatures  $T_{x1}$  and  $T_{x2}$  for the heating rate 5 and 10K/min are:  $T_{x1}=680$  and  $692 \text{ K}$  and  $T_{x2}=819$  and  $824 \text{ K}$ , respectively.

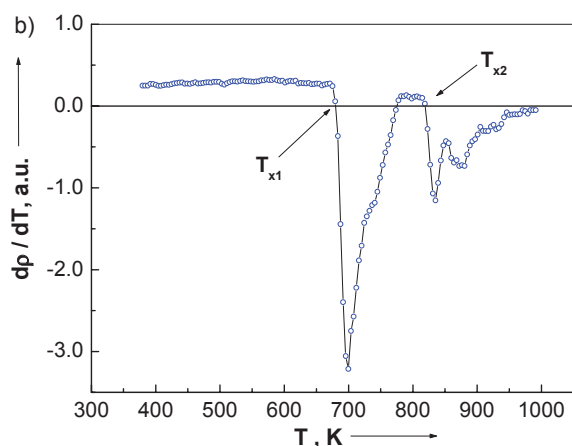
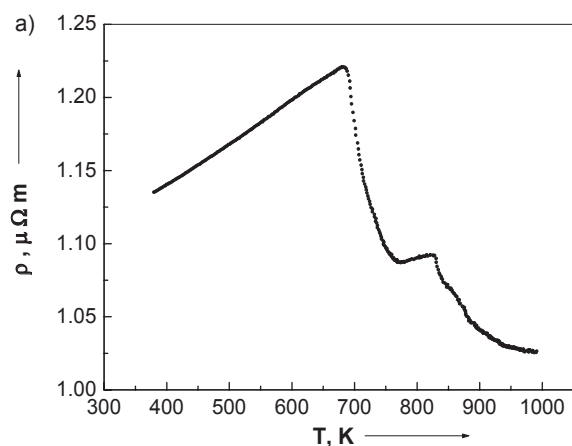


Fig. 6. Electrical resistivity  $\rho(T)$  measured with heating rate 5 K/min for the  $\text{Co}_{80}\text{Si}_9\text{B}_{11}$  alloy (a) and (b) the  $d\rho/dT$  curve for the data presented in (a)

Fig 8, 9 a and Fig. 8, 9 b presents a family of magnetization curves  $M(T)$  normalized to the value at 300 K (heating rate  $\nu=5$  and 10 K/min) and the corresponding  $dM/dT$  curves, respectively. The characteristic temperature  $T_{x1}$  is determined from the condition  $dM/dT$  maximum and is about 725 and 730 K for the heating rate 5 and 10 K/min, respectively. The value of  $T_{x1}$  deduced in this way corresponds to the highest formation rate of the new ferromagnetic phase. With increasing heating rate the maxima of  $dM/dT$  shift towards higher temperatures which is characteristic feature of thermally activated (diffusion controlled) process [25].

From the results presented in Fig. 8 and 9 it can be seen that the formation of  $\text{Co}_2\text{B}$  phase is quite noticeable in  $\text{Co}_{80}\text{Si}_9\text{B}_{11}$  alloy as indicated by the arrow [26].

First stage of crystallization was found in 723 K for the  $\text{Co}_{80}\text{Si}_9\text{B}_{11}$  alloy heat-treated for 0.5 and 1.0 h (Fig. 1, Table 3). The phases formed in different heat treatment conditions were identified using XRD, as in Fig. 1 in Table 3.

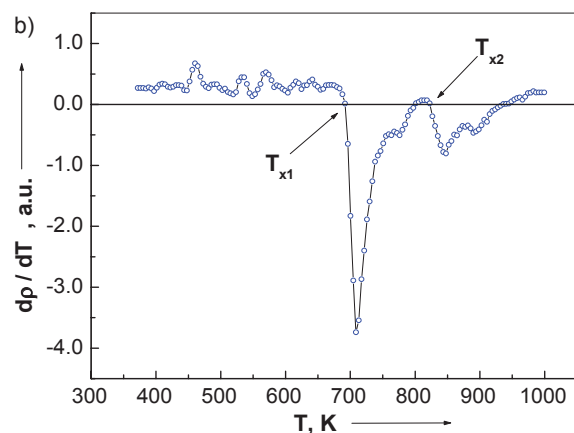
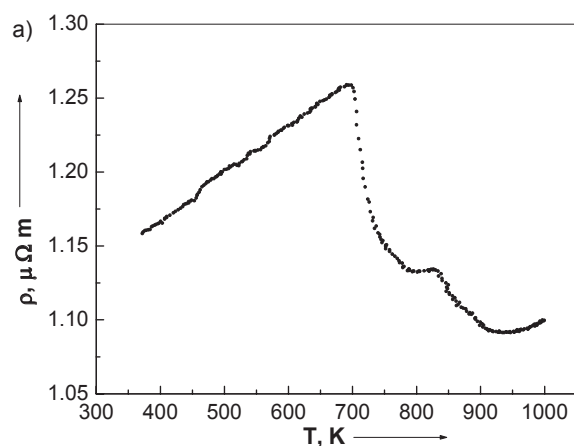


Fig. 7. Electrical resistivity  $\rho(T)$  measured with heating rate 10 K/min for the  $\text{Co}_{80}\text{Si}_9\text{B}_{11}$  alloy (a) and (b) the  $d\rho/dT$  curve for the data presented in (a)

Further increase of annealing temperature leads to changes in X-ray diffraction (Fig. 1) and at annealing temperature 773 K the  $\alpha\text{-Co}$ ,  $\text{Co}_2\text{Si}$  and  $\text{Co}_3\text{B}$  phases was identified. Samples heat-treated at 748 and 773 K (Fig. 1) for 0.5 and 1.0 h has similar phases. As can be seen from Figure 1 at 748 K the crystallization of the amorphous alloy proceeds through nucleation of the hexagonal (h.c.p.)  $\alpha\text{-Co}$  phase in the amorphous matrix. For samples heat-treated for 0.5 and 1.0 h at temperature 873 K  $\text{Co}_2\text{B}$  phase appear (Fig. 1, table 3). There are sharp changes in the intensity of the phases formed at higher temperature and longer time.

Additionally for the samples heat-treated at 873 K for 1 h the structure investigation performed by XRD method using diffractometer's parameters – Table 1 (b). The aim of this investigation was found existence/non-existence the body-centered cubic (bcc)  $\beta\text{-Co}$  phase. The diffraction pattern (Fig. 10) did not indicate (bcc)  $\beta\text{-Co}$  phase in the samples annealed at 873 K for 1 h.

Table 2.

The parameters of heat treatment (temperature and time) and initial relative magnetic permeability  $\mu_r$  of the Co<sub>80</sub>Si<sub>9</sub>B<sub>11</sub> alloy

Annealing temperature $T_a$ , K	The initial relative magnetic permeability $\mu_r$ of Co <sub>80</sub> Si <sub>9</sub> B <sub>11</sub> alloy after	
	0.5 h annealing	1.0 h annealing
aq <sup>1)</sup>	1090	1090
373	1049	1056
423	916	1361
473	850	942
523	875	611
573	528	1073
623	531	445
673	361	581
723	589	798
748	120	145
773	65	69
823	58	56
873	57	56

<sup>1)</sup> - as quenched state

The obtained of experimental data shows that the values of crystallization temperature  $T_{x1}$  obtained from magnetization measurements and from resistivity curves are not the same [27,29]. This difference cannot be explained neither by the unavoidable temperature gradient existing in both apparatuses nor by the natural dependence of magnetization on temperature [25].

Based on investigation results the value of the crystallization temperature  $T_{x1}$  of an amorphous Co<sub>80</sub>Si<sub>9</sub>B<sub>11</sub> is strongly depend on the heat treatment conditions (linear heating or isothermal heating) and on the using methods. Using different methods the compare the value of the crystallization temperature  $T_{x1}$  can take place only under a constant heating rate.

The changes of structure and magnetic properties have been observed with increasing the temperature annealing of investigated alloy in range 373÷873 K by 0.5 and 1.0 h (Fig. 1, 2, 6-10, Table 2, 3) [14].

Initial magnetic permeability  $\mu_r$  measured as a function of annealing temperature  $T_a$ . From Table 2 it can be recognized that the investigated alloy annealed for 0.5 and 1.0 h in temperature range 373÷723 K the  $\mu_r$  has high value, i.e. 1049÷589 and 1056÷798, respectively.

It can be recognized that the heat treatment of Co<sub>80</sub>Si<sub>9</sub>B<sub>11</sub> alloy (at temperature  $T_a > T_{x1}$ ) initial relative magnetic permeability  $\mu_r$  passes by a distinct maximum related to formation of nanocrystalline phase  $\alpha$ -Co, Co<sub>3</sub>B and Co<sub>2</sub>Si. Increase of annealing temperature leads to further decrease of initial relative magnetic permeability  $\mu_r$  (Table 2) which can be related to the formation of boride Co<sub>2</sub>B besides mentioned phases [14,24].

The structural instability alloy in the amorphous and nanocrystalline phases leads to anomalies in the dependence of the magnetic properties on temperature [27]. In amorphous ribbons, a number of physical properties change due to

structural relaxations. It is known that amorphous alloy annealing below the crystallization temperature relaxes the residual internal stresses induced during the preparation process, improving the magnetic response of the material. Higher temperatures of annealing initiate the crystallization process in the amorphous alloy [17,29].

Table 3.

The phase analysis results for the Co<sub>80</sub>Si<sub>9</sub>B<sub>11</sub> alloy annealed at  $T_a=773$  and 873 K by 0.5 and 1.0 h (see Fig. 1)

d, Å	$\alpha$ -Co	$d_\alpha$ (hkl) Co <sub>3</sub> B	for Co <sub>2</sub> B	phases: Co <sub>2</sub> Si
2.500			2.510 (200)	
2.340		2.363 (112)		
2.165*	2.165 (100)			
2.130		2.128 (121)		2.130 (310)
2.100			2.113 (002)	
2.030*	2.023 (002)	2.031 (210)		2.020 (220)
2.000				2.000 (301)
1.980		1.975 (103)	1.983 (211)	1.970 (121)
1.940*		1.942 (211)		
1.910*	1.910 (101)			
1.870		1.860 (122)		1.870 (002)
1.850		1.848 (113)		1.850 (311)
1.800			1.815 (112)	
1.740		1.732 (212)		
1.700				1.700 (112)
1.660*		1.657 (004)		1.670 (410)
1.616		1.620 (130)	1.616 (202)	
1.590			1.588 (310)	1.600 (130)
1.485	1.480 (102)			
1.250*	1.252 (110)			1.250 (412)
1.187			1.192 (213)	1.190 (113)
1.179			1.183 (330)	
1.167			1.169 (411)	
1.149*	1.149 (103)			
1.105				1.110 (023)
1.101				1.100 (512)
1.083	1.083 (200)			
1.065*	1.066 (112)			
1.046*	1.047 (201)			1.050 (341)
1.031				1.032 (332)
1.016*	1.015 (004)			
0.987			0.973 (204)	

d – lattice parameters calculated from Fig. 1

$d_\alpha$  – lattice parameters of identified phases [28]

\* - the peak appearing in Co<sub>80</sub>Si<sub>9</sub>B<sub>11</sub> alloy annealed at  $T_a=773$  K by 0.5 and 1.0 h, too

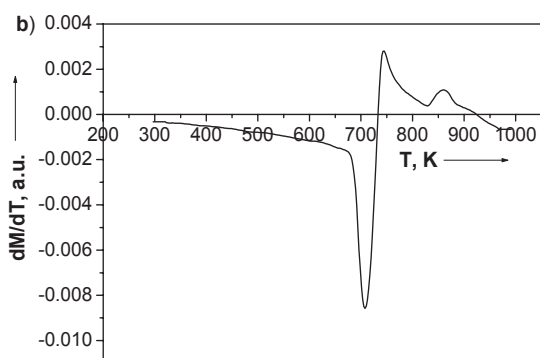
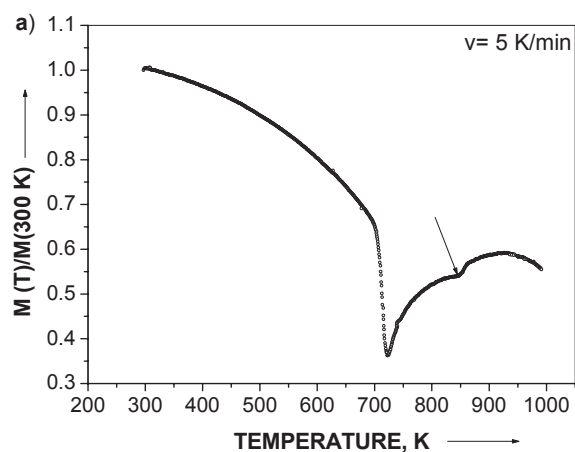


Fig. 8. Normalized magnetization versus temperature  $T$  of  $\text{Co}_{80}\text{Si}_9\text{B}_{11}$  alloy (a) and (b) -  $dM/dT$  curves for the data presented in (a)

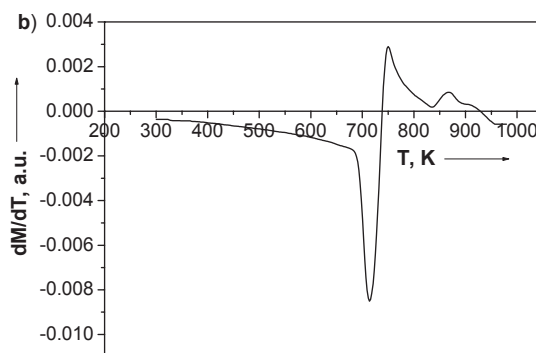
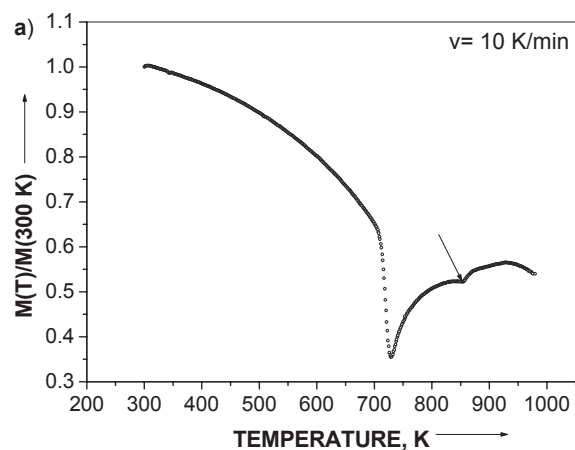


Fig. 9. Normalized magnetization versus temperature  $T$  of  $\text{Co}_{80}\text{Si}_9\text{B}_{11}$  alloy (a) and (b) -  $dM/dT$  curves for the data presented in (a)

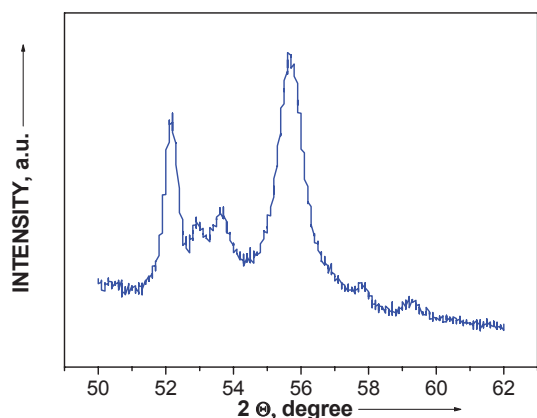


Fig. 10. X-ray diffraction pattern of the  $\text{Co}_{80}\text{Si}_9\text{B}_{11}$  alloy after annealing at temperature  $T_a=873\text{K}$  for 1.0 h. The parameters of diffractometer – see Table 1 (b)

## 4. Conclusions

The crystallization behaviour of the  $\text{Co}_{80}\text{Si}_{11}\text{B}_9$  metallic glasses is studied using different methods. The main conclusion of the paper can be summarized as follows: Amorphous  $\text{Co}_{80}\text{Si}_9\text{B}_{11}$  type alloy is not in thermodynamic equilibrium state as a consequence of rapid cooling from the liquid phase. Production process causes the time and thermal instabilities of physical (magnetic and electric) properties of this material. These instabilities are reduced by thermal annealing. It can be explained by structural relaxation connected with annealing out of free volume frozen during rapid cooling and crystallization of material. After annealing at elevated temperatures, the  $\alpha$ -Co phase is formation. For higher annealing temperatures the  $\text{Co}_3\text{B}$  and  $\text{Co}_2\text{Si}$  phases are formed, it causes a strongly decrease of relative magnetic permeability.

The activation energy of crystallization process obtained by Kissinger method is  $3.0 \pm 0.2$  eV. The value is similar for the high cobalt alloys in all cases.

## Additional information

The presentation connected with the subject matter of the paper was presented by the authors during the 14<sup>th</sup> International Scientific Conference on Achievements in Mechanical and Materials Engineering AMME'2006 in Gliwice-Wisła, Poland on 4<sup>th</sup>-8<sup>th</sup> June 2006.

## References

- [1] T.Y. Byun, Y. Oh, C.S. Yoon, C.K. Kim, Crystallization and magnetic properties of  $(\text{Co}_{0.75}\text{Cr}_{0.25})_{80}\text{Si}_5\text{B}_{15}$  metallic glass, *Journal of Alloys and Compounds* 368 (2004) 283-286.
- [2] I.C. Rho, C.S. Yoon, C.K. Kim, T.Y. Byun, K.S. Hong, Crystallization of amorphous alloy CoFeCrSiB, *Materials Science and Engineering B96* (2002) 48-52.
- [3] T. Gloriant, S. Surinach, M.D. Baró, Stability and crystallization of Fe-Co-Nb-B amorphous alloys, *Journal of Non-Crystalline Solids* 333 (2004) 320-326.
- [4] D. Szewieczek, J. Tyrlik – Held, S. Lesz, Changes of fracture morphology of amorphous tapes involved by crystallization process, *Proceedings of the Scientific Conference Materials and Manufacturing M<sup>3</sup>E'2000, Gliwice, 2000*, 267-272.
- [5] P. Gramatyka, R. Nowosielski, P. Sakiewicz, Magnetic properties of polymer bonded nanocrystalline polder, *Journal of Achievements in Materials and Manufacturing Engineering* 20, (2007) 115-118.
- [6] B. Ziębowicz, D. Szewieczek, L.A. Dobrzański, New possibilities of application of composite materials with soft magnetic properties, *Journal of Achievements in Materials and Manufacturing Engineering* 20 (2007) 207-210.
- [7] J. Konieczny, L.A. Dobrzański, A. Przybył, J. Wysłocki, Structure and magnetic properties of powder soft magnetic materials, *Journal of Achievements in Materials and Manufacturing Engineering* 20 (2007) 139-142.
- [8] R. Nowosielski, L.A. Dobrzański, J. Konieczny, Influence of temperature on structure and magnetic properties of powders alloys, *Journal of Achievements in Materials and Manufacturing Engineering* 20 (2007) 163-166.
- [9] M. Wen, M. Zhong, K.E. J. Wu, L. Li, H. Qi, S. Cao, T. Zhang, Soft magnetic Co-Fe-B-P and Co-Fe-V-B-P amorphous alloy nano-particles prepared by aqueous chemical reduction, *Journal of Alloys and Compounds* 417 (2006) 245-249.
- [10] S. Mudry, B. Kotur, L. Bednarska, Y. Kulyk, A. Korolyshyn, O. Hertsyk, The formation of intermetallic phases upon crystallization of amorphous alloys  $\text{Co}_{67.2}\text{Fe}_{3.8}\text{Cr}_{3.0}\text{Si}_{14.0}\text{B}_{12.0}$  and  $\text{Co}_{66.5}\text{Fe}_{4.0}\text{Mo}_{1.5}\text{Si}_{16.0}\text{B}_{12.0}$ , *Journal of Alloys and Compounds* 367 (2004) 274-276.
- [11] R. Hasegawa, Advances in amorphous and nanocrystalline magnetic materials, *Journal of Magnetism and Magnetic Materials* 304 (2006) 187-191.
- [12] P. Vojtanik, Magnetic relaxations in amorphous soft magnetic alloys, *Journal of Magnetism and Magnetic Materials* 304 (2006) 159-163.
- [13] T. Misu, A. Sugiura, M. Kanazawa, S. Hamada, T. Kusaka, K. Sato, K. Katsuki, High-permeability cobalt-based amorphous core for the use of an untuned broadband RF cavity, *Nuclear Instruments and Methods in Physics Research A* 557 (2006) 383-389.
- [14] S. Lesz, R. Nowosielski, A. Zajdel, B. Kostrubiec, Z. Stokłosa, Structure and magnetic properties of the amorphous  $\text{Co}_{80}\text{Si}_9\text{B}_{11}$  alloy, *Journal of Achievements in Materials and Manufacturing Engineering* 18 (2006) 155-158.
- [15] R. Nowosielski, A. Zajdel, A. Baron S. Lesz, Influence of crystallization an amorphous  $\text{Co}_{77}\text{Si}_{11.5}\text{B}_{11.5}$  alloy on corrosion behavior, *Journal of Achievements in Materials and Manufacturing Engineering* 20 (2007) 167-170.
- [16] H. Matyja, T. Kulik, *Proceedings of the 3<sup>rd</sup> International Workshop on Non-Crystalline Solids, Trends in Non Crystalline Solids, Matalascanas (Costa De LA Luz), Spain, World Scientific Pub Co Inc, 1991.*
- [17] H. Chiriac, C. Hison, Influence of laser irradiation on magnetic properties of Co-Fe-Si-B amorphous ribbons, *Materials Science and Engineering A304-306* (2001) 1066-1068.
- [18] Y. Yoshizawa, K. Yamauchi, S. Oguma, *European Patent Application 0 271 657 (22.06.1988)*
- [19] D. Dróżdż, T. Kulik, The effect of preannealing conditions on the crystallization behaviour of amorphous  $\text{Co}_{78}\text{Si}_{11}\text{B}_{11}$ , *Materials Engineering* 4 (2001) 283-285.
- [20] J. Rasek, *Some diffusion phenomena in crystalline and amorphous metals, Silesian University Press, Katowice 2000.* (in Polish)
- [21] P. Kwapuliński, A. Chrobak, G. Haneczok, Z. Stokłosa, J. Rasek, J. Lelaćko, Optimization of soft magnetic properties in nanoperm type alloys, *Materials Science and Engineering C* 23 (2003) 71-75.
- [22] H.E. Kissinger, *Analytical Chemistry* 29 (1957) 1702.
- [23] P. Kwapuliński, J. Rasek, Z. Stokłosa, G. Haneczok, Magnetic properties of amorphous and nanocrystalline alloys based on iron, *Journal of Materials Processing Technology* 157-158 (2004) 735-742.
- [24] L.F. Barquín, J.M. Barandiarán, I. Tellería, J.C. Gómez Sal, A comparative study of the crystallization of Co-Si-B metallic glasses, *Journal of Magnetism and Magnetic Materials* 160 (1996) 297-298.
- [25] A. Chrobak, D. Chrobak, G. Haneczok, P. Kwapuliński, Z. Kwolek, M. Karolus, Influence of Nb on the first stage of crystallization in  $\text{Fe}_{86-x}\text{Nb}_x\text{B}_{14}$  amorphous alloys, *Materials Science and Engineering A* 382 (2004) 401-406.
- [26] C-S. Yoo, S.K. Lim, C.S. Yoon, C.K. Kim, Effect of Pt addition on the crystallization of Co-based amorphous metallic alloys, *Journal of Alloys and Compounds* 359 (2003) 261-266.
- [27] G. Bordin, G. Buttino, A. Cecchetti, M. Poppi, Temperature dependence of magnetic properties of a Co-based alloy in amorphous and nanocrystalline phase, *Journal of Magnetism and Magnetic Materials* 195 (1999) 583-587.
- [28] R. Jenkins, W.F. McClune, T.M. Maguire, et al., *Powder Diffraction Data, JCPDS – International Centre for Diffraction Data, 1601 Parklane, Swarthmore, PA 19081, USA, 1986.*
- [29] S. Lesz, Formation of the nanocrystalline structure by controlling crystallization of amorphous Fe-Hf-B alloy, doctoral desirtation in Polish, Gliwice, Poland, 2001 (in Polish).